Journal of King Saud University – Science 35 (2023) 102388

HOSTED BY

Contents lists available at ScienceDirect

Journal of King Saud University – Science

journal homepage: www.sciencedirect.com

Original article

Electron-hole recombination effect of SnO_2 – CuO nanocomposite for improving methylene blue photocatalytic activity in wastewater treatment under visible light

V. Perumal [a], R. Uthrakumar [a,*], M. Chinnathambi [b], C. Inmozhi [c], R. Robert [b], M.E. Rajasaravanan [a], A. Raja [d], K. Kaviyarasu [e,f,*]

[a] Department of Physics, Govt. Arts College (Autonomous), Salem 636007, Tamil Nadu, India
[b] Department of Physics, Govt. Arts College for Men, Krishnagiri 635001, Tamil Nadu, India
[c] Department of Physics, Govt. Arts College for Women, Salem 636008, Tamil Nadu, India
[d] Department of Chemistry, College of Natural Sciences, Yeungnam University, Gyeongsan, Republic of Korea
[e] UNESCO-UNISA Africa Chair in Nanosciences/Nanotechnology Laboratories, College of Graduate Studies, University of South Africa (UNISA), Muckleneuk Ridge, PO Box 392, Pretoria, South Africa
[f] Nanosciences African Network (NANOAFNET), Materials Research Group (MRG), iThemba LABS-National Research Foundation (NRF), 1 Old Faure Road, 7129, PO Box 722, Somerset West, Western Cape Province, South Africa

ARTICLE INFO

Article history:
Received 11 June 2022
Revised 15 September 2022
Accepted 17 October 2022
Available online 27 October 2022

Keywords:
SnO_2 – CuO heterostructure
Photodegradation
Electron-hole pair recombination
Electron microscopy
Heterojunction photocatalysts
Visible light irradiation

ABSTRACT

Heterojunction photocatalysts have gained much attraction in pollutant degradation applications due to their unique good adsorption and photocatalytic decomposition capacity and more cycle durability. Tin oxide (SnO_2) doped with copper oxide (CuO) heterostructured photocatalyst was synthesized by a simple solution processes technique. X-ray diffraction and fluorescence spectroscopy were used to examine the structural properties of the SnO_2 - CuO heterostructure. Analyses of FE-SEM and TEM were performed on the samples to determine their surface morphology. The photodegradation property of SnO_2 - CuO heterostructure was studied using methylene blue (MB) model pollutant, where SnO_2 - CuO heterostructure (90.3 % at 180 min) was shown better than the SnO_2. Therefore, the *n-p*-junction (SnO_2 - CuO) heterostructure catalysis boosted the photodegradation of MB detailed studies on the electron-hole pair recombination were conducted on *n-p*-junctions to observe the effect of the interface on the recombination have been published.

1. Introduction

The fast industrialization and civilization process is creating the most hazardous pollution in the environment. Water pollution is one of the major concerns of eco-friendly environments (Kaviyarasu et al., 2012). Water pollution did not only create serious health impacts and have changed the lifestyle of water-living organisms (Perumal et al., 2022). Further, the premature deaths counts were increased day by day owing to the water pollution (Kasinathan et al., 2016). The recycling or purification of textiles, food, paint, and leather industries wastes (organic pollutant) are challenging task, because are it easily mixed with water resource (Chandrasekar et al., 2021). Research communities are much interested to develop the fast, highly efficient, and low-cost degradation method (*physical, chemical, and biological*). Among them, solar-driven semiconductor - based photocatalysis technology have gained much attention owing to the simple, eco-friendly, and can decomposed the organic pollutants without secondary products (Arularasu et al., 2018; Panimalar et al., 2020; Amal George et al., 2022). The different semiconductor materials were used for photocatalysts process such as metal oxide (Geetha et al., 2018; Panimalar et al., 2022; Raja et al., 2019; Perumal et al., 2022), transition metal sulfide (Panimalar et al., 2022; Chandrasekar et al.,

* Corresponding authors at: UNESCO-UNISA Africa Chair in Nanosciences/Nanotechnology Laboratories, College of Graduate Studies, University of South Africa (UNISA), Muckleneuk Ridge, PO Box 392, Pretoria, South Africa (K. Kaviyarasu).
E-mail addresses: uthraloyola@yahoo.com (R. Uthrakumar), kavi@tlabs.ac.za (K. Kaviyarasu).

Peer review under responsibility of King Saud University.

Production and hosting by Elsevier

https://doi.org/10.1016/j.jksus.2022.102388
1018-3647/

2022; Manjula et al., 2018; Amanulla et al., 2021), carbon-based materials (Thirupathy et al., 2020; Kayalvizhi et al., 2022; Subbareddy et al., 2020; Alhaji et al., 2019), and metal-organic frameworks (MOFs). Among them, metal oxide widely investigated for photocatalytic field, which owing to the high chemical stability, low toxic nature, wide bandgap, and large exaction biding energy. Most of semiconductors metal oxide only absorbs UV lights only, which limited the practical application. The combination of two metal oxides was not only cover the visible and UV spectra, also boosted the photocatalytic properties.

The use of metal oxide nanostructures in electronics, optics, and photonics systems has gained wide attention because of their wide bandgaps (3.7 eV) and large exciton binding energies (60 meV) (Kennedy et al., 2017; Fang et al., 2014; Murmu et al., 2021). Among them, SnO_2 and CuO heterojunction were formed the *n-p*-junction, which was boosted the photocatalytic properties due to their high photosensitivity, reduce the recombination rate, non-toxic nature, and large bandgap. SnO_2 is wide bandgap *n*-type semiconductor (3.7 eV) and CuO is a *p*-type semiconductor (1.5 eV). In *n-p*-heterojunction, CuO was acts as a sink, where it helps to sperate the electron-hole pair (reduced the recombination) and the photogenerated electrons-holes pair move in the opposite direction, get gather in the valence band of SnO_2 and efficiently pairs of electrons and holes recombine less frequently. Due to the low recombination of (*high movement of electron in the opposite direction*) SnO_2 - CuO heterostructure, the photocatalytic property of SnO_2 - CuO heterostructure will be improved (George et al., 2022; Kumar et al., 2016). In this study, SnO_2 - CuO heterostructured photocatalyst was synthesized by a simple solution processes method. The as structural, optical, morphology were thoroughly characterized by XRD, UV–vis spectroscopy, FESEM and EDX. As MB dye degradation was illuminated with UV light, the catalysts were measured for their activity. The photocatalytic activities in the degradation of high concentrated malachite green dyes have been investigated in detailed.

2. Experimental

2.1. Materials

Copper acetate tetrahydrate ($Cu(CO_2CH_3)_2{\cdot}4H_2O$), tin chloride pentahydrate ($SnCl_4{\cdot}5H_2O$), sodium hydroxide (NaOH), Polyvinylpyrrolidone (PVP), Ethanol (C_2H_5OH) purchasing was done through Sisco Research Laboratories Pvt. ltd, India. No further purification was performed on the chemicals.

2.2. Synthesis method of SnO_2 - CuO heterostructured photocatalyst

SnO_2 - CuO heterostructured photocatalyst was synthesized by a simple solution processes method. Initially, 1:1 ratio of copper acetate tetrahydrate and tin chloride pentahydrate were added in 100 mL deionized (DI) water and stirrer 1 h. In addition to the clear solution, PVP was added in 0.1 g and stirred for 15 min. Then, 1.5 g of sodium hydroxide was dissolved 50 mL and sodium hydroxide solution gradually added the above homogeneous solution. Several times, DI water and ethanol were used to wash the precipitate. A final annealing at 400 °C for 3 hrs in an air atmosphere was followed by a drying at 80 °C overnight. The product was noted as SnO_2 - CuO. For comparison, SnO_2 and CuO were also synthesized under the same reaction condition without copper acetate tetrahydrate and tin chloride pentahydrate, respectively.

2.3. Characterization techniques

The crystalline structure of as-synthesized sample was characterized by X-ray diffractometer (XRD) (AERIS high-resolution bench top) with CuK_α radiation. The morphology and energy dispersive X-ray spectroscopy (EDX) of SnO_2 - CuO was investigated by FE-SEM (Thermo scientific Apreo S) with an acceleration voltage of 20 kV and TEM (JEOL Japan, JEM-2100 Plus) with an acceleration voltage of 200 kV. μ-Raman vibration modes of as synthesized samples were examined by Raman spectrometer (HORIBA France, LABRAM HR Evolution) at green (532 nm) laser light. The optical absorption properties of the samples were performed by UV–vis-DRS SHIMADZU, UV 3600 PLUS analysis, to evaluate the optical properties of the samples.

2.4. Photocatalytic studies

By degrading organic pollutants under visible light, SnO_2 - CuO heterostructured catalysts were evaluated for their photocatalytic properties. We stirred 50 mL of DI water for 15 min with 10 ppm of methylene blue (MB) dye and 10 ppm of magnesium blue (MB) dye. Then, 50 mg of SnO_2 - CuO heterostructured catalyst was added the above solution and stirred 20 min under the dark condition. An under visible light irradiated 10 cm away from the surface of the solution was then used to expose the model pollutant with catalyst. The organic pollutant solution was collected each 30 min and studied the UV–vis absorption spectrum. The decomposition rate of each catalyst was studied by following equation (Abinaya et al., 2018).

$$D(\%) = \frac{C_0 - C_t}{C_0} \times 100 \quad (1)$$

3. Results and discussion

3.1. XRD pattern

The SnO_2 sample (Fig. 1) shows the diffraction peaks at 25.38°, 33.81°, 38.91°, 51.55°, 54.37°, 57.93°, 61.46°, 64.75° and 65.61° are assigned to (110), (101), (200), (210), (211), (220), (002), (310), (112) and (301) planes, respectively. It was matched with tetragonal rutile structure (JCPDS card no. 41–1445). It appears that CuO diffraction peaks are located at 32.51°, 35.55°, 38.72°, 48.75°, 53.48°, 58.25°, 61.51°, 66.21°, and 68.07°, which correspond to planes as follows: (110), (002), (111), (−202), (020), (202), (−113), (−311), and (220). All the peaks are well-matched with the monoclinic CuO (JCPDS card no. 48–1548). Further composite the SnO_2 and CuO, there was no significant changes in the diffraction pattern, which could be attributed to the formation SnO_2 - CuO nanocomposite (Mariammal et al., 2012).

3.2. μ-Raman spectrum

The vibration mode of SnO_2 - CuO composite was analyzed by μ-Raman analysis as shown in Fig. 2. The peaks located at 633 cm^{-1} and 779 cm^{-1} could be assigned to the (A_{1g}) symmetric and (B_{2g}) asymmetric stretching of Sn-O bonds, respectively. The peak at ~ 569 cm^{-1} represent (E_g) doubly degenerate mode of oxygen ions in SnO_2. In CuO sample was observed with three peaks at 295, 345, and 625 cm^{-1}, which are assigned to the A_g mode (oxygen vibrations along the crystallographic *b*-axis), B_{1g} mode (*a*-axis

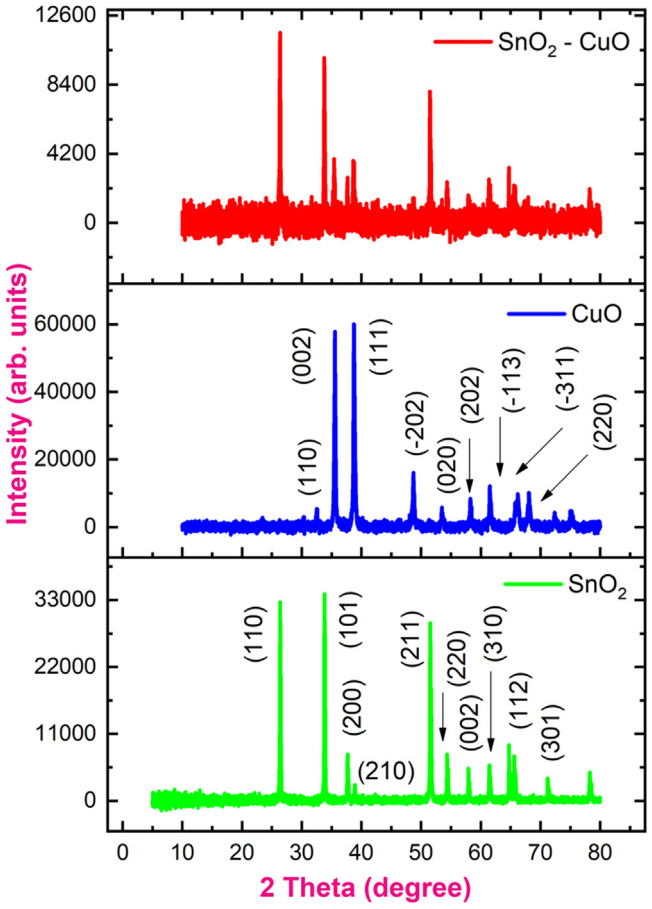

Fig. 1. XRD pattern of samples containing SnO_2, CuO, and SnO_2 - CuO nanocomposites.

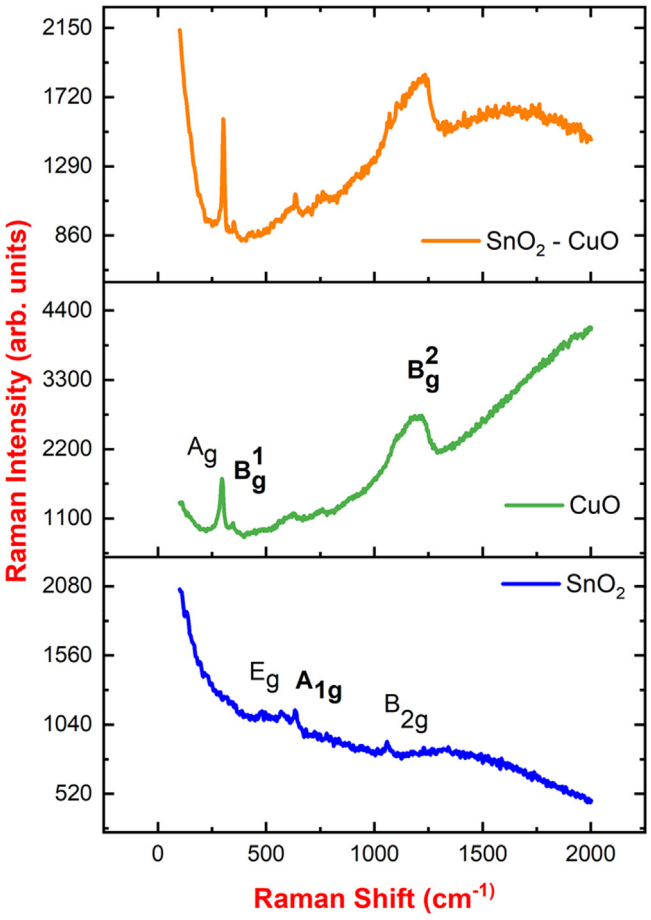

Fig. 2. μ-Raman spectrum of SnO_2, CuO, and SnO_2 - CuO nanocomposite samples.

vibrations of oxygen), and B_{2g} mode (oxygen vibrations perpendicular to the b-axes). Thus, the presence of SnO_2 and CuO in the composites were confirmed from the μ-Raman spectroscopy (Kumar et al., 2021).

3.3. FTIR analysis

The functional properties of SnO_2, CuO and SnO_2 - CuO heterostructure sample were studied by FTIR analysis as shown in Fig. 3. At 3433 cm^{-1}, a broad band was observed; it was attributed to the stretching vibration of water molecules in the O—H direction. Due to the presence of PVP in the SnO_2 - CuO heterostructure, two more-absorption bands were observed at 2927 cm^{-1} and 1388 cm^{-1}, which correspond to N—H and C—H vibrations. There are two peaks at 620 cm^{-1} and 580 cm^{-1} corresponding to Sn-O and Cu–O vibrations, respectively. The most inorganic metal–oxygen (M–O) stretching modes were observed 700 cm^{-1} to 400 cm^{-1}. From the FTIR analysis, the presence and formation of SnO_2 - CuO heterostructure were confirmed (Joshi et al., 2016; Wang et al., 2018).

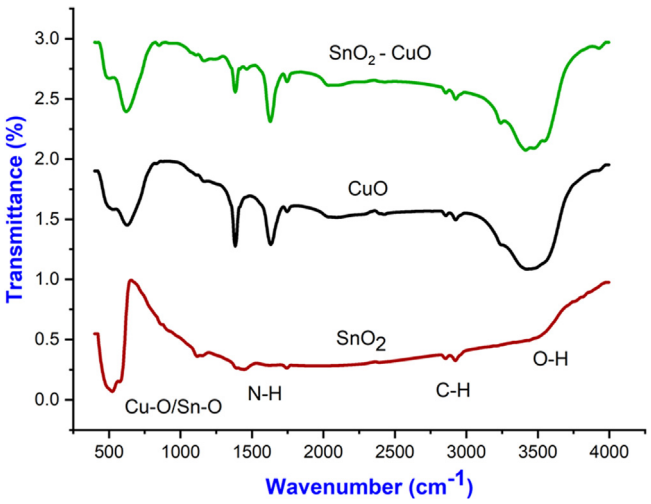

Fig. 3. FTIR spectrum of SnO_2, CuO, and SnO_2 - CuO nanocomposite samples.

3.4. UV–vis analysis

The optical absorption and optical bandgap of SnO_2, CuO and SnO_2 - CuO heterostructure samples as shown in Fig. 4(a-c). Within the 200 nm to 800 nm wavelength range of pure SnO_2, CuO, and SnO_2 - CuO samples were studied for their optical absorption spectra. The SnO_2 and CuO samples exhibited an absorption edge around ~400 and 800 nm, respectively. When combination with SnO_2 and CuO (*heterostructure*), the intermediate absorption edge was observed at 500 nm. The shift indicates that the introduction of a new energy level presence in the bandgap. The energy bandgap values have been calculated by *Kubelka-Munk*. At any wavelength, the *Kubelka-Munk* function is given by equation 2 and 3.

$$\frac{\alpha}{S} = F(R) = \frac{(1-R)^2}{2R} \quad (2)$$

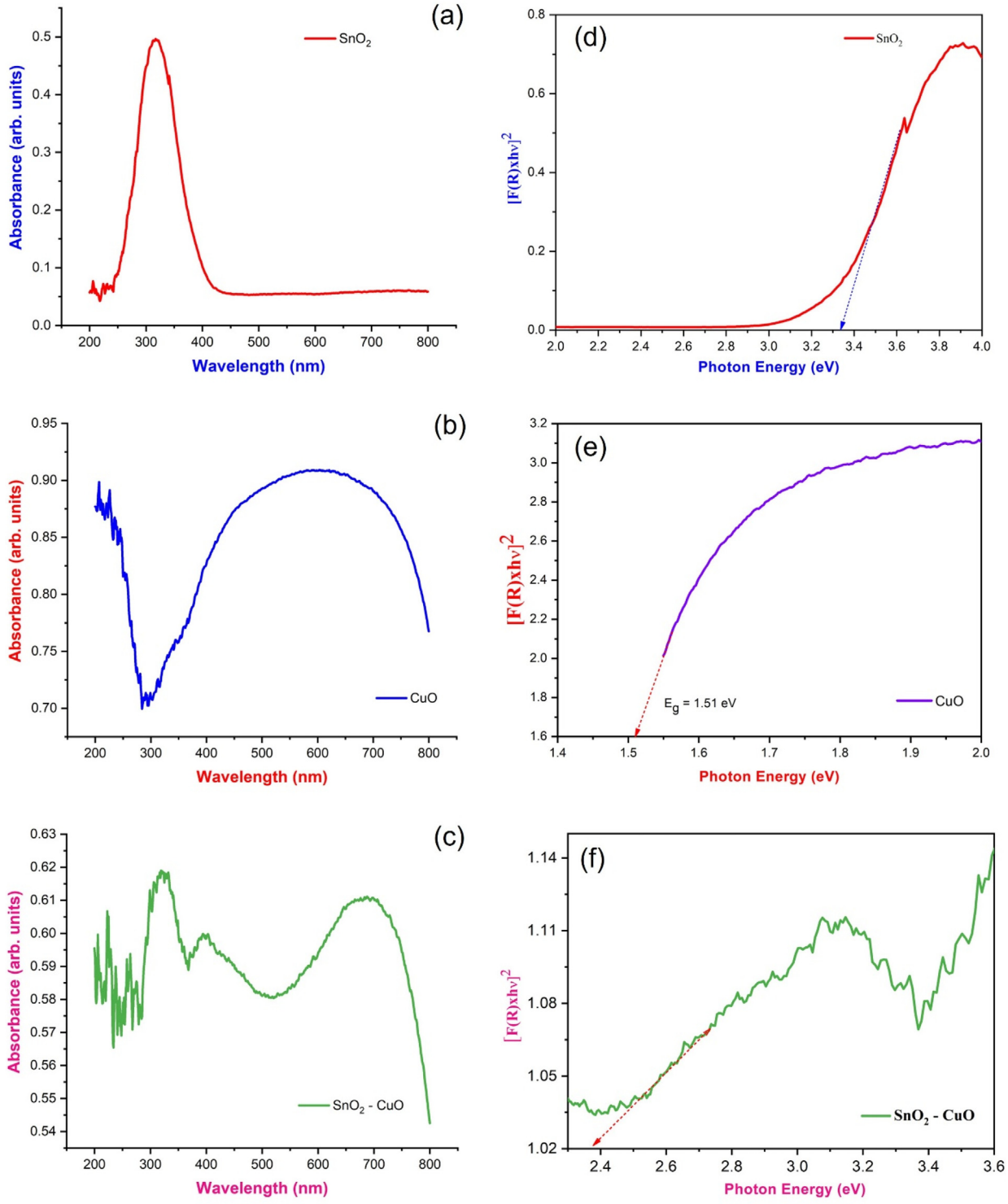

Fig. 4. (a-c) UV–vis absorption spectrum of SnO_2, CuO, and SnO_2 - CuO samples and; (d-f) bandgap energy of SnO_2, CuO, and SnO_2 - CuO samples.

$$R = \frac{R_{Sample}}{R_{Standard}} \quad (3)$$

'α' is the absorption coefficient, 'S' is the scattering coefficient, and *F(R) is the (K-M) Kubelka Munk function*. The bandgap of SnO_2, CuO and SnO_2 - CuO samples were found to be 3.36 eV, 1.51 eV, and 2.3 eV, respectively as shown in inset Fig. 4(d-f). This new energy level was increasing the photocatalytic properties (Harish et al., 2016).

3.5. Morphology analysis

The morphology of SnO_2 - CuO heterostructures were analyzed by FESEM techniques. As shown in Fig. 5(a-f), SnO_2, CuO and SnO_2 - CuO heterostructure samples exhibit different morphologies. The FESEM image of SnO_2 in Fig. 5(a-b) shows rock-like morphology and it agglomerated. In Fig. 5(c-d) shows the FESEM image of CuO, which was nanoparticles matrix. In fact, the FESEM images

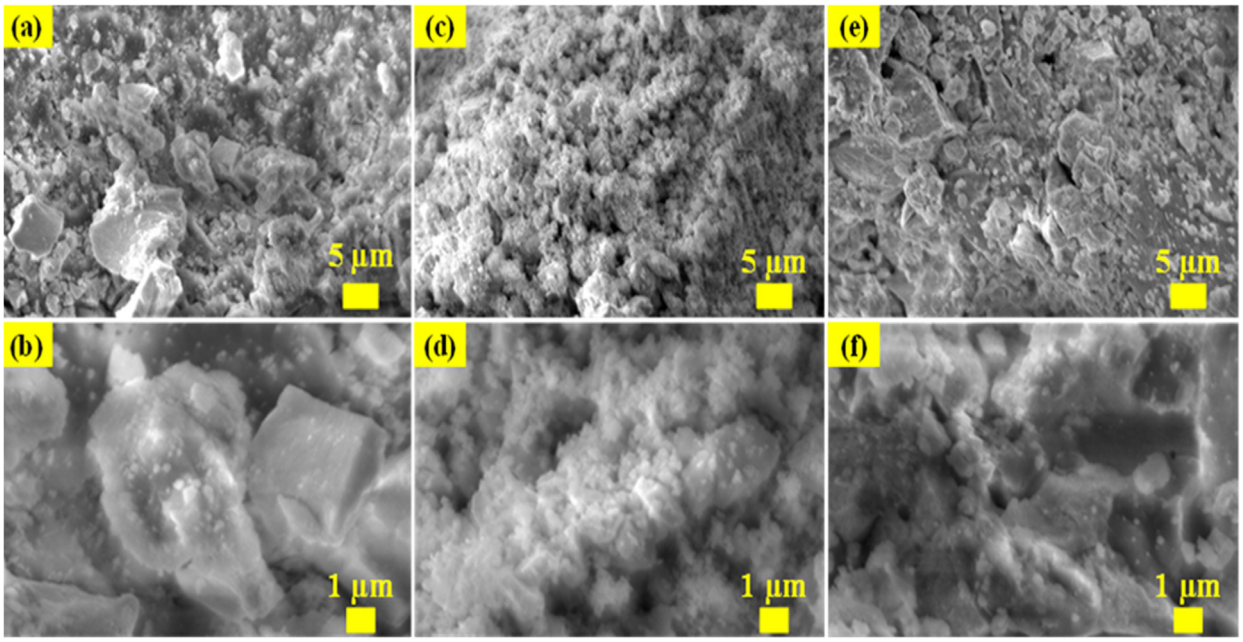

Fig. 5. (a-b) FESEM images of SnO_2; (c-d) CuO; and (e-f) SnO_2 - CuO nanocomposite samples.

of SnO_2 - CuO heterostructures revealed that the sample was rock-like, and nanoparticles morphology was bunch of *rock-like* and nanoparticles aggregated together to form an irregular morphology as shown in Fig. 5(e-f) respectively.

The illustration shows TEM images of Fig. 6(a-b) SnO_2 - CuO heterostructure, the TEM results were in good agreement with FESEM (rock-like and nanoparticles morphology). Based on the TEM images of SnO_2 - CuO, the clear lattice fringes were observed, which is due to the good crystalline nature of SnO_2 - CuO nanocomposite. Nevertheless, smaller particles contain grain boundaries, which work as barriers to the passage of free carriers and traps for carriers. Furthermore, the elemental distribution mapping of SnO_2 - CuO was characterized by FESEM analysis with EDX mapping as shown in Fig. 7(a-d). The Sn, Cu and O elements were uniform distribution of rock-like SnO_2 - CuO heterostructure, where it confirmed SnO_2 - CuO in (rock-like and nanoparticles morphology structure) (Panimalar et al., 2022; Magdalane et al., 2021; Subash et al., 2022).

3.6. Photocatalytic activity

The photocatalytic property of SnO_2 - CuO heterostructures were analyzed using MB model pollutant. The UV absorption spectrum of model pollutant was revealed in the Fig. 8(a-d). The degradation rate of MB was calculated from the UV–vis absorption spectra and the calculated percentage of SnO_2, CuO, and SnO_2 - CuO was 58 %, 62.2 %, and 90.3 %, respectively as shown in Fig. 8 (a). In the dark condition, a negligible amount of decomposition was observed, and it as shown in Fig. 8(b). The SnO_2 - CuO heterostructure shows much better performance under light irradiation when compared with other samples, which is owing to heterojunction as shown in Fig. 8(c). The optimum concentration of Cu has formed the heterojunction, which increases the trap state in the heterojunction and reduced the recombination rate of electrons (e^-) and holes (h^+). The Fig. 8(d) (energy band diagram of the SnO_2 - CuO heterostructure) shows possible photodegradation mechanism of MB. From photodegradation mechanism scheme,

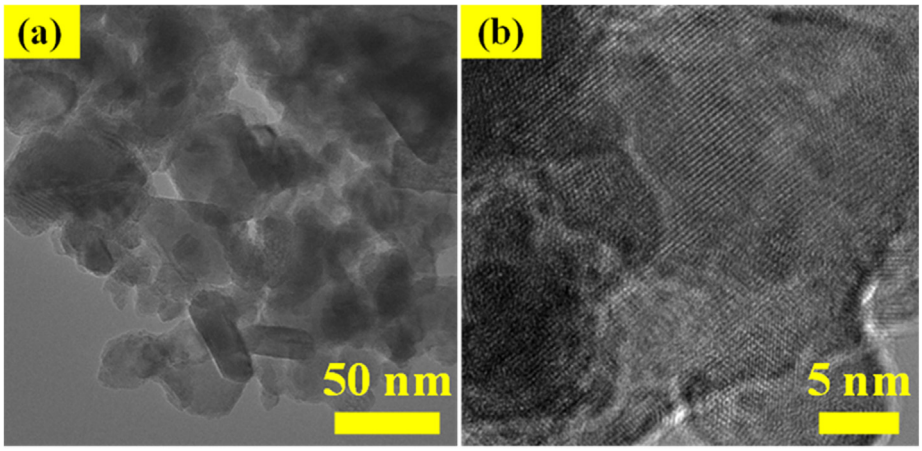

Fig. 6. (a-b). TEM images of SnO_2 - CuO nanocomposite sample.

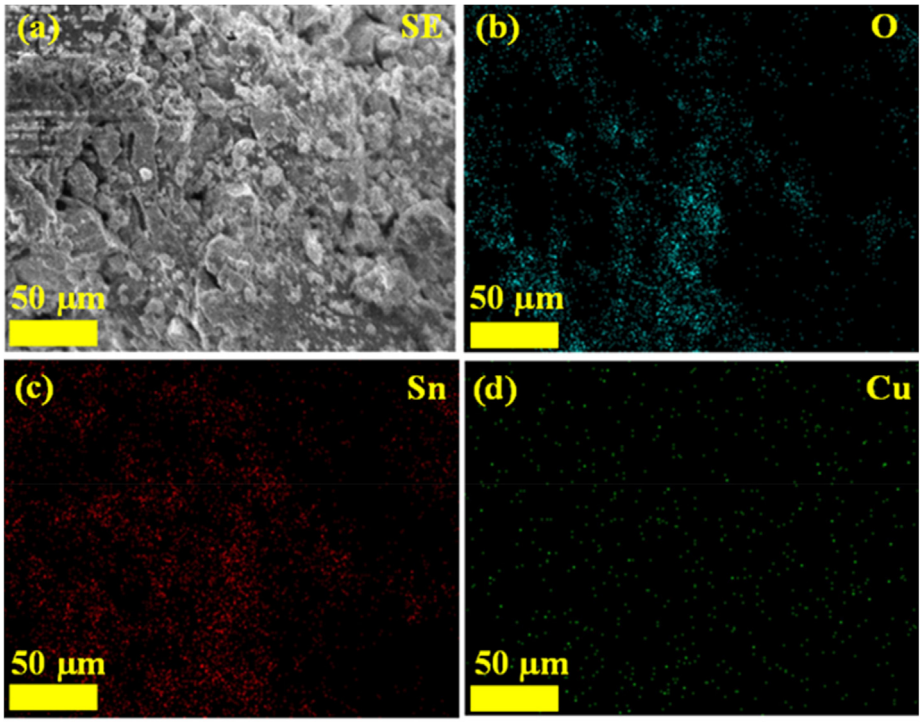

Fig. 7. (a-d). FESEM and EDX mapping of SnO_2 - CuO nanocomposite sample.

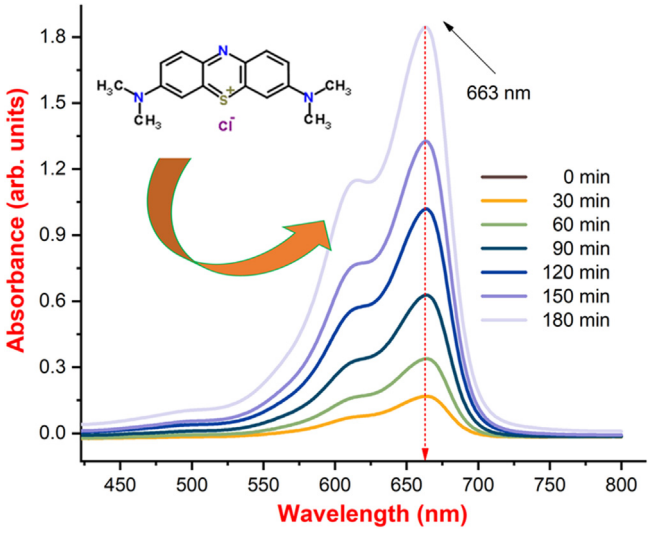

Fig. 8(a). Absorption spectrum of SnO_2 - CuO heterostructure samples as a function of MB dye degradation efficiency.

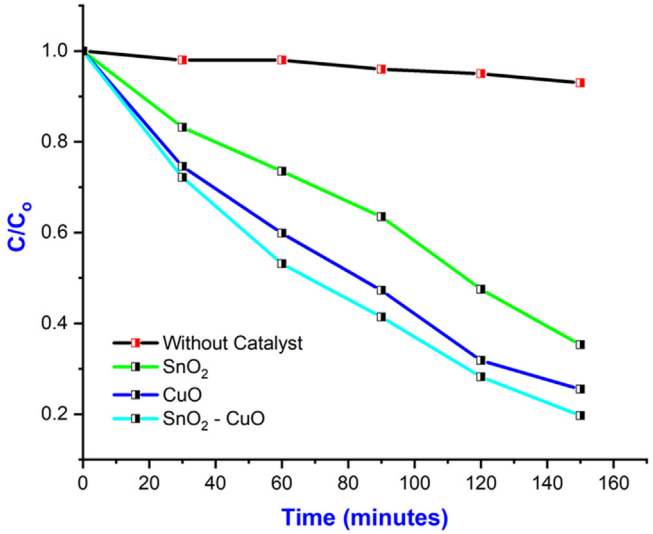

Fig. 8(b). Degradation efficiency of C/C_o vs time (different concentration) of SnO_2, CuO, and SnO_2 - CuO heterostructure samples.

the SnO_2 - CuO heterostructure absorbed the photons from the electromagnetic radiation and electron - hole (e^-/h^+) pair create in the heterojunction. The electrons generated by photogeneration were transferred from the CB of CuO to the CB of SnO_2. It is important for dye solution degradation to produce highly reactive radical ions, including hydroxyl radicals (OH^-) and superoxide radical ions ($^{\bullet}O_2$).

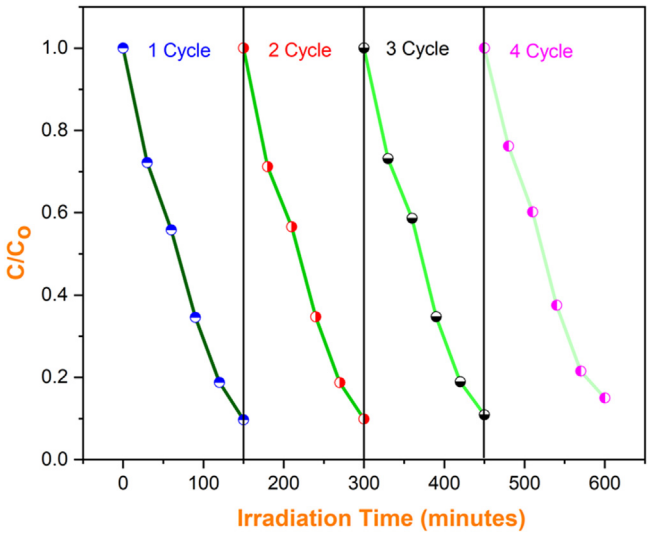

Fig. 8(c). Reusability of SnO_2 - CuO photocatalyst under light irradiation

$$H_2O + h^+ \rightarrow H^+ + OH^+ (\text{Oxidation})$$

$$O_2 + e^- \rightarrow O_2^- (\text{Reduction})$$

These defect levels operate as active sites for the photocatalytic response because photo-generated electrons and holes can be trapped by oxygen and surface hydroxyl species. In CuO, electron-hole pairs were separated after the hole was transferred from the VB of SnO_2. Hydroxide radicals ($OH^\bullet$) were formed from $OH^\bullet$ as $OH^\bullet$ was being reduced. In this reaction, the super radicals reacted with each other and gave off H_2O as a yield. These highly active species ultimately oxidize CO_2 and H_2O by generating either photogenerated electrons or holes from reactive hydroxide radicals with high oxidation abilities (Roguai and Djelloul, 2022; Begum et al., 2022).

4. Conclusion

The SnO_2 - CuO heterostructure was synthesized by a simple solution processes technique. The physical properties of SnO_2 - CuO heterostructure were deliberate by XRD and μ-Raman analysis, where the exhibits of SnO_2 and CuO were confirmed. The presences of SnO_2 and CuO in heterojunction were confirmed from the FESEM with EDX analysis. In fact, the photodegradation activity of SnO_2 - CuO heterostructure were studied by using MB model pollutant, where SnO_2 - CuO heterostructure was degrades 90.3 % amount of highly reactive with MB in 180 min and convert into inactive some other radicals. Though, the degradation percentage of SnO_2 - CuO heterostructure was high when compared with other sample due to the high catalytic and low recombination rate of *n*-*p*-heterojunctions was calculated to be 90.3 %. Water and wastewater treatment can utilize the SnO_2 - CuO heterostructure to decompose emerging pollutants using visible light.

Declaration of Competing Interest

The authors declare that they have no known competing financial interests or personal relationships that could have appeared to influence the work reported in this paper.

Acknowledgements

In their acknowledgement, the authors express their gratitude to the management team. The authors also appreciate the support and encouragement of Yeungnam University, Gyeongsan, Republic of Korea.

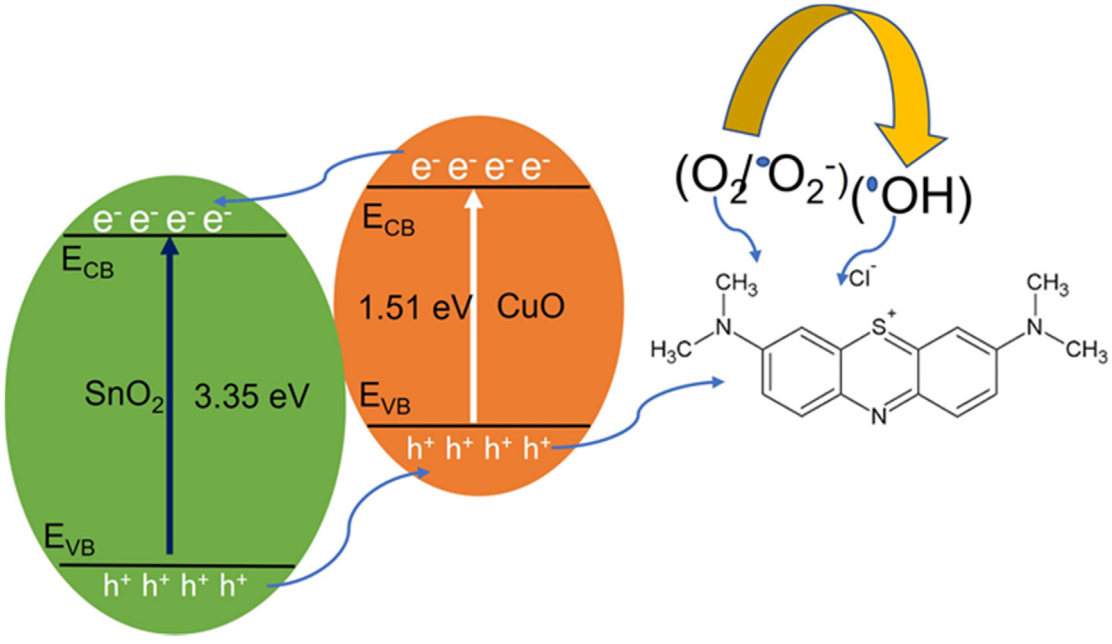

Fig. 8(d). Fig. 8(d). A schematic illustration of the photocatalytic mechanism for the heterojunction SnO_2 - CuO nanoparticles

References

Abinaya, R., Archana, J., Harish, S., Navaneethan, M., Ponnusamy, S., Muthamizhchelvan, C., Shimomura, M., Hayakawa, Y., 2018. Ultrathin layered MoS_2 nanosheets with rich active sites for enhanced visible light photocatalytic activity. RSC Adv. 8, 26664.

Alhaji, N.M.I., Nathiya, D., Kaviyarasu, K., Meshram, M., Ayeshamariam, A., 2019. A comparative study of structural and photocatalytic mechanism of $AgGaO_2$ nanocomposites for equilibrium and kinetics evaluation of adsorption parameters. Surf. Interfaces 17, 100375.

Amal George, D., Raj, M.A., Venci, X., Dhayal Raj, A., Albert Irudayaraj, A., Josephine, R.L., John Sundaram, S., Al-Mohaimeed, A.A., Al, D.A., Farraj, T.-W., Kaviyarasu, K., 2022. Photocatalytic effect of CuO nanoparticles flower-like 3D nanostructures under visible light irradiation with the degradation of methylene blue (MB) dye for environmental application. Environ. Res. 203, 111880.

Amanulla, A.M., Magdalane, C.M., Saranya, S., Sundaram, R., Kaviyarasu, K., 2021. Selectivity, stability and reproducibility effect of CeM-CeO_2 modified PIGE electrode for photoelectrochemical behaviour of energy application. Surf. Interfaces 22, 100835.

Arularasu, M.V., Anbarasu, M., Poovaragan, S., Sundaram, R., Kanimozhi, K., Maria Magdalane, C., Kaviyarasu, K., Thema, F.T., Letsholathebe, D., Mola, G.T., Maaza, M., 2018. Structural, optical, morphological, and microbial studies on SnO_2 nanoparticles prepared by co-precipitation method. J. Nanosci. Nanotechnol. 18 (5), 3511–3517.

Begum, S., Ranjan Mishra, S., Md, 2022. Ahmaruzzaman, Facile synthesis of NiO-SnO_2 nanocomposite for enhanced photocatalytic degradation of bismarck brown. Inorg. Chem. Commun. 143, 109721.

Chandrasekar, M., Panimalar, S., Uthrakumar, R., Kumar, M., Raja Saravanan, M.E., Gobi, G., Madheswaran, P., Inmozhi, C., Kaviyarasu, K., 2021. Preparation and characterization studies of pure and Li^+ doped ZnO nanoparticles for optoelectronic applications. Materials Today: Proceedings 36, 228–231.

Chandrasekar, M., Subash, M., Perumal, V., Panimalar, S., Aravindan, S., Uthrakumar, R., Inmozhi, C., Isaev, A.B., Sudhakar Muniyasamy, A., Raja, K., 2022. Kaviyarasu Specific charge separation of Sn doped MgO nanoparticles for photocatalytic activity under UV light irradiation. Sep. Purif. Technol. 294, 121189.

Fang, F., Kennedy, J., Carderb, D., Futter, J., Rubanov, S., 2014. Investigations of near infrared reflective behaviour of TiO_2 nanopowders synthesized by arc discharge. Opt. Mater. 36, 1260–1265.

Geetha, N., Sivaranjani, S., Ayeshamariam, A., Siva Bharathy, M., Nivetha, S., Kaviyarasu, K., Jayachandran, M., 2018. High performance photo-catalyst based on nanosized ZnO - TiO_2 nanoplatelets for removal of RhB under visible light irradiation. J. Adv. Microsc. Res. 13 (1), 12–19.

George, A., Dhayal Raj, A., Albert Irudayaraj, A., Josephine, R.L., Venci, X., John Sundaram, S., Rajakrishnan, R., Kuppusamy, P., Kaviyarasu, K., 2022. Regeneration study of MB in recycling runs over nickel vanadium oxide by solvent extraction for photocatalytic performance for wastewater treatments. Environ. Res. 211, 112970.

Harish, S., Archana, J., Navaneethan, M., Silambarasan, A., Nisha, K.D., Ponnusamy, S., Muthamizhchelvan, C., Ikeda, H., Aswal, D.K., Hayakawa, Y., 2016. Enhanced visible light induced photocatalytic activity on the degradation of organic pollutant by SnO nanoparticles decorated hierarchical ZnO nanostructures. RSC Adv. 6, 89721.

Joshi, S., Ippolito, S.J., Sunkara, M.V., 2016. Convenient Architectures of Cu_2O/SnO_2 Type II *p-n* Heterojunctions and their Application in Visible Light Catalytic Degradation of Rhodamine. Blue RSC Adv. 6, 43672.

Kasinathan, K., Kennedy, J., Elayaperumal, M., Henini, M., Malik, M., 2016. Photodegradation of organic pollutants RhB dye using UV simulated sunlight on ceria based TiO_2 nanomaterials for antibacterial applications. Sci. Rep. 6 (1), 1–12.

Kaviyarasu, K., Devarajan, P.A., Xavier, S.S.J., Thomas, S.A., Selvakumar, S., 2012. One pot synthesis and characterization of cesium doped SnO_2 nanocrystals via a hydrothermal process. J. Mater. Sci. Technol. 28 (1), 15–20.

Kayalvizhi, K., Alhaji, N.M.I., Saravanakkumar, D., Beer Mohamed, S., Kaviyarasu, K., Ayeshamariam, A., Al-Mohaimeed, A.M., AbdelGawwad, M.R., Elshikh, M.S., 2022. Adsorption of copper and nickel by using sawdust chitosan nanocomposite beads–A kinetic and thermodynamic study. Environ. Res. 203, 111814.

Kennedy, J., Fang, F., Futter, J., Leveneur, J., Murmu, P.P., Panin, G.N., Kang, T.W., Manikandan, E., 2017. Synthesis and enhanced field emission of zinc oxide incorporated carbon nanotubes. Diam. Relat. Mater. 71, 79–84.

Kumar, M.P., Murugadoss, G., Mangalaraja, R.V., Kumar, M.R., 2021. Enhanced electrocatalytic activity of CuO-SnO_2 nanocomposite in alkaline medium. Appl. Phys. A Mater. Sci. Process. 127, 1.

Kumar, A., Rout, L., Achary, L.S.K., Mohanty, A., Marpally, J., Chand, P.K., Dash, P., 2016. Design of Binary SnO_2-CuO Nanocomposite for Efficient Photocatalytic Degradation of Malachite Green Dye. AIP Conf. Proc. 12, 1724.

Magdalane, C.M., Priyadharsini, G.M.A., Kaviyarasu, K., Jothi, A.I., Simiyon, G.G., 2021. Synthesis and characterization of TiO_2 doped cobalt ferrite nanoparticles via microwave method: investigation of photocatalytic performance of Congo red degradation dye. Surf. Interfaces 25, 101296.

Manjula, N., Kaviyarasu, K., Ayeshamariam, A., Selvan, G., Diallo, A., Ramalingam, G., Mohamed, S.B., Letsholathebe, D., Jayachandran, M., 2018. Structural, morphological and methanol sensing properties of jet nebulizer spray pyrolysis effect of TiO_2 doped SnO_2 thin film for removal of heavy metal ions. Journal of Nanoelectronics and Optoelectronics 13 (10), 1543–1551.

Mariammal, R.N., Ramachandran, K., Renganathan, B., Sastikumar, D., 2012. On the enhancement of ethanol sensing by CuO modified SnO_2 nanoparticles using fiber-optic sensor. Sensors Actuators, B Chem. 169, 199.

Murmu, P.P., Shettigar, A., Chong, S.V., Liu, Z., Goodacre, D., Jovic, V., Mori, T., Smith, K.E., Kennedy, J., 2021. Role of phase separation in nanocomposite indium-tin-oxide films for transparent thermoelectric applications. Journal of Materiomics 7, 612–620.

Panimalar, S., Uthrakumar, R., Tamil Selvi, E., Gomathy, P., Inmozhi, C., Kaviyarasu, K., Kennedy, J., 2020. Studies of MnO_2/g-C_3N_4 hetrostructure efficient of visible light photocatalyst for pollutants degradation by sol-gel technique. Surf. Interfaces 20, 100512.

Panimalar, S., Subash, M., Chandrasekar, M., Uthrakumar, R., Inmozhi, C., Al-Onazi, W.A., Al-Mohaimeed, A.M., Tse-Wei Chen, J., Kennedy, M., Maaza, K.K., 2022. Reproducibility and long-term stability of Sn doped MnO_2 nanostructures: Practical photocatalytic systems and wastewater treatment applications. Chemosphere 293, 133646.

Panimalar, S., Chandrasekar, M., Logambal, S., Uthrakumar, R., Inmozhi, C., 2022. Europium-doped MnO_2 nanostructures for controlling optical properties and visible light photocatalytic activity. Mater. Today:. Proc. 56, 3394–3401.

Panimalar, S., Logambal, S., Thambidurai, R., Inmozhi, C., Uthrakumar, R., Muthukumaran, A., Rasheed, R.A., Gatasheh, M.K., Raja, A., Kennedy, J., Kaviyarasu, K., 2022. Effect of Ag doped MnO_2 nanostructures suitable for wastewater treatment and other environmental pollutant applications. Environ. Res. 205, 112560.

Perumal, V., Sabarinathan, A., Chandrasekar, M., Subash, M., Inmozhi, C., Uthrakumar, R., Isaev, A.B., Raja, A., Elshikh, M.S., Almutairi, S.M., Kaviyarasu, K., 2022. Hierarchical nanorods of graphene oxide decorated SnO_2 with high photocatalytic performance for energy conversion applications. Fuel 324, 124599.

Perumal, V., Inmozhi, C., Uthrakumar, R., Robert, R., Chandrasekar, M., Beer Mohamed, S., Shehla Honey, A., Raja, F.h.A., Al-Mekhlafi, K.K., 2022. Enhancing the photocatalytic performance of surface - Treated SnO_2 hierarchical nanorods against methylene blue dye under solar irradiation and biological degradation. Environ. Res. 209, 112821.

Raja, A., Selvakumar, K., Rajasekaran, P., Arunpandian, M., Ashokkumar, S., Kaviyarasu, K., Asath Bahadur, S., Swaminathan, M., 2019. Colloids Surf., A 564 (5), 23–30.

Roguai, S., Djelloul, A., 2022. Elaboration, characterization and applications of SnO_2, 2 %Gd-SnO_2 and 2 %Gd-9 %F-SnO_2 thin films for the photocatalytic degradation of MB by USP method. Inorg. Chem. Commun. 138, 109308.

Subash, M., Chandrasekar, M., Panimalar, S., Inmozhi, C., Parasuraman, K., Uthrakumar, R., Kaviyarasu, K., 2022. Pseudo-first kinetics model of copper doping on the structural, magnetic, and photocatalytic activity of magnesium oxide nanoparticles for energy application. Biomass Conversion and Biorefinery 12, 1–11.

Subbareddy, Y., Naresh Kumar, R., Sudhakar, B.K., Rayappa Reddy, K., Martha, S.K., Kaviyarasu, K., 2020. A facile approach of adsorption of acid blue 9 on aluminium silicate-coated Fuller's Earth - Equilibrium and kinetics studies. Surf. Interfaces 19, 100503.

Thirupathy, C., Lims, S.C., Sundaram, S.J., Mahmoud, A.H., Kaviyarasu, K., 2020. Equilibrium synthesis and magnetic properties of $BaFe_{12}O_{19}/NiFe_2O_4$ nanocomposite prepared by co precipitation method. Journal of King Saud University-Science 32 (2), 1612–1618.

Wang, K., Zhang, W., Lou, F., Wei, T., Qian, Z., Guo, W. J. Solid State Electrochem. Preparation of electrospun heterostructured hollow SnO_2/CuO nanofibers and their enhanced visible light photocatalytic performance 22, (2018) 2413.